

Phase noise of dispersion-managed solitons

Elaine T. Spiller^{1,2} and Gino Biondini^{1,*}

¹*Department of Mathematics, State University of New York at Buffalo, Buffalo, New York 14260, USA*

²*Department of Mathematics, Statistics and Computer Science, Marquette University, Milwaukee, Wisconsin 53201, USA*

(Received 11 March 2009; published 21 July 2009)

We quantify noise-induced phase deviations of dispersion-managed solitons (DMS) in optical fiber communications and femtosecond lasers. We first develop a perturbation theory for the dispersion-managed nonlinear Schrödinger equation (DMNLSE) in order to compute the noise-induced mean and variance of the soliton parameters. We then use the analytical results to guide importance-sampled Monte Carlo simulations of the noise-driven DMNLSE. Comparison of these results with those from the original unaveraged governing equations confirms the validity of the DMNLSE as a model for many dispersion-managed systems and quantify the increased robustness of DMS with respect to noise-induced phase jitter.

DOI: [10.1103/PhysRevA.80.011805](https://doi.org/10.1103/PhysRevA.80.011805)

PACS number(s): 42.65.-k, 05.40.-a, 05.45.Yv

I. INTRODUCTION

The performance of many light wave systems is ultimately limited by quantum noise. Scientifically and technologically important examples include optical fiber communication systems and femtosecond (fs) lasers: the former are a key enabling technology for the information age, while Ti:sapphire fs lasers have applications to optical atomic clocks. Estimating the performance of these systems is a timely problem. Because both kinds of systems are designed to operate with very high accuracies, however, failures result from the occurrence of unusually large deviations, which makes calculating error rates extremely difficult. Direct Monte Carlo (MC) computations of failure rates are impractical due to the exceeding number of samples necessary to obtain reliable estimates, and analytical predictions are impossible due to the scale and the complexity of these systems. In particular, errors in both systems are often phase sensitive, and both systems employ the technique of dispersion management, whereby pulses propagate through a periodic concatenation of components with opposite signs of dispersion [1,2]. The probability of rare events can often be efficiently calculated using importance sampling (IS), with which the noise is sampled from a biased distribution that makes the rare events occur more frequently. For IS to be successful, however, one must bias toward the most likely noise realizations that lead to the events of interest. For systems modeled by the nonlinear Schrödinger equation (NLSE), this is made possible using soliton perturbation theory (SPT) [3–6], but this tool is not available in dispersion-managed (DM) systems. Recently [7], we developed a perturbation theory for the dispersion-managed NLSE (DMNLSE) that governs the long-term dynamics of DM optical systems [8–10], and we performed importance-sampled MC (ISMC) simulations of the pulse amplitude and frequency. Here, we employ this perturbation theory in order to compute noise-induced means and variances, and we develop IS for the DMNLSE by explicitly formulating and solving the optimal biasing problem. We then perform ISMC simulations of the pulse phase, where the choice of biasing is nontrivial. Finally, we com-

pare these results to the original unaveraged system as well as to systems with constant dispersion.

II. PERTURBATIONS OF DM SOLITONS

The propagation of optical pulses in dispersion-managed fiber communication systems [1] and Ti:sapphire lasers [2] is described by an equation which we refer to as NLSE+DM,

$$i(\partial q/\partial z) + (1/2)d(z/z_a)(\partial^2 q/\partial t^2) + g(z/z_a)|q|^2 q = i\nu(t, z). \quad (1)$$

Here, z is the propagation distance, t is the retarded time, $q(t, z)$ is the slowly varying electric field envelope (rescaled to account for loss and amplification), $d(z/z_a)$ is the local dispersion, and $g(z/z_a)$ describes the periodic power variation due to loss and amplification. The choice of $d(z/z_a)$ is called a dispersion map and z_a is the dispersion map period. The forcing is $\nu(t, z) = \sum_{n=1}^{N_a} \nu_n(t) \delta(z - nz_a)$, where $\delta(z)$ is the Dirac delta and $\nu_n(t)$ is the white Gaussian noise, satisfying $\mathbb{E}[\nu_n(t)] = 0$ and $\mathbb{E}[\nu_n(t)\nu_n^*(t')] = \sigma\delta(t-t')\delta_{nn'}$, where $\mathbb{E}[\cdot]$ denotes ensemble average, the asterisk denotes complex conjugation, $\delta_{nn'}$ is the Kronecker delta, and σ^2 is the noise variance.

Once the compression and expansion of the pulse in each dispersion map is properly factored out, the core pulse shape obeys the DMNLSE [8–10]. Namely, to the leading order we, can approximate the solution of Eq. (1) as $\hat{q}(\omega, z, \zeta) = e^{-iC(\zeta)\omega^2/2}\hat{u}(\omega, z)$, where $\hat{f}(\omega) = \int e^{-i\omega t} f(t) dt$ is the Fourier transform of $f(t)$ (all integrals are complete unless limits are given) and $\zeta = z/z_a$. Here $C(\zeta) = z_a \int_0^\zeta [d(\zeta') - \bar{d}] d\zeta'$, where \bar{d} is the average dispersion. The exponential factor in front of $\hat{u}(\omega, z)$ accounts for the rapid “breathing,” while the slowly varying envelope $\hat{u}(\omega, z)$ satisfies the perturbed DMNLSE

$$i(\partial u/\partial z) + (1/2)\bar{d}(\partial^2 u/\partial t^2) + \int \int u_{(t+t')} u_{(t+t'')}^* R_{(t', t'')} dt' dt'' = i\nu(t, z), \quad (2)$$

where the asterisk denotes complex conjugate and for brevity $u_{(i)} = u(t, z)$, etc. The kernel $R(t', t'')$ quantifies the average nonlinearity over a dispersion map mitigated by dispersion management: $R(t', t'') = \int \int e^{i\omega' t' + i\omega'' t''} r(\omega', \omega'') d\omega' d\omega''$, where $r(x) = \int_0^1 e^{ixC(\zeta)} g(\zeta) d\zeta$.

The DMNLSE and its solutions depend on a parameter s ,

*biondini@buffalo.edu

called the *reduced map strength*, which quantifies the size of the dispersion variations around their mean. Dispersion-managed solitons (DMSs) are traveling-wave solutions of the DMNLSE. If $u_o(t, z; s) = e^{i\lambda^2 z/2} f(t; s)$, then $\hat{f}(\omega)$ satisfies a nonlinear integral equation which can be efficiently solved numerically [7]. The invariances of the DMNLSE then yield from $u_o(t, z; s)$ a four-parameter family of DMS,

$$u_{\text{DMS}}(t, z; s) = e^{i\Theta(t, z)} A f(A(t-T); A^2 s), \quad (3)$$

where A and Ω are the DMS amplitude and frequency, $\Theta(t, z) = \Omega(t-T) + \Phi$ is the local phase, and T and Φ are, respectively, the mean time and the mean phase. In the unperturbed case, the mean time and the mean phase evolve according to $\dot{T} = \Omega$ and $\dot{\Phi} = (A^2 + \Omega^2)/2$. (Hereafter, the overdot denotes differentiation with respect to z .)

In the presence of perturbations, the DMS will evolve. If $u(t, z) = u_{\text{DMS}} + w$ solves the noise-perturbed DMNLSE, $w(t, z)$ satisfies the corresponding perturbed linearized DMNLSE. But part of the noise goes to change the soliton parameters. The noise-induced DMS parameter that changes at each map period are found by demanding that $w(t, z)$ remains small, and are written as $Q(nz_a^+) = Q(nz_a^-) + \Delta Q$, where for $Q = A, \Omega, T$ it is $\Delta Q = \langle e^{i\Theta} \underline{y}_Q, \nu_n(t) \rangle / \langle \underline{y}_Q, \underline{y}_Q \rangle$, while [7]

$$\Delta \Phi = \langle e^{i\Theta} \underline{y}_\Phi, \nu_n(t) \rangle / \langle \underline{y}_\Phi, \underline{y}_\Phi \rangle + \Omega \langle e^{i\Theta} \underline{y}_T, \nu_n(t) \rangle / \langle \underline{y}_\Omega, \underline{y}_\Omega \rangle. \quad (4)$$

Here, $\langle f, g \rangle = \text{Re} \int f^*(t) g(t) dt$ is the inner product; $y_A(t), \dots, y_\Phi(t)$ are the neutral and the generalized eigenmodes of the linearized DMNLSE; and $\underline{y}_A(t), \dots, \underline{y}_\Phi(t)$ are the adjoint modes [7]: $y_T = -\partial U / \partial \xi$, $y_\Omega = i \xi U$,

$$y_\Phi = iU, \quad y_A = \frac{1}{A} [U + \xi(\partial U / \partial \xi) + 2s(\partial U / \partial s)], \quad (5)$$

while $y_\Phi = i y_A$, $y_T = -i y_\Omega / A$, $y_\Omega = -y_T / A$, and $\underline{y}_A = U$. Here $\xi = t - T(z)$ and $U(t, z) = u(t, z) e^{-i\Theta}$ is the DMS envelope. All of these results reduce to those arising from soliton perturbation theory for the NLSE [4] when $s=0$.

III. NOISE-INDUCED PARAMETER VARIANCES

When the perturbation in Eq. (2) represents noise, the above results yield a system of nonlinear stochastic differential equations (SDEs) for the evolution of the DMS parameters under the effect of noise,

$$\dot{Q} = \nu_Q(z), \quad \dot{\Phi} = \frac{1}{2}(A^2 + \Omega^2) + \Omega \nu_T(z) + \nu_\Phi(z) \quad (6)$$

for $Q = A, \Omega, T$, where the source terms are $\nu_Q(z) = \langle e^{i\Theta} \underline{y}_Q, S \rangle / \langle \underline{y}_Q, \underline{y}_Q \rangle$ for all Q . We employ a continuum approximation of Eqs. (6), considering $\nu(t, z)$ to be a zero-mean Gaussian white-noise process with autocorrelation $\mathbb{E}[S(t, z) S^*(t', z')] = \sigma^2 \delta(t-t') \delta(z-z')$. The sources $\nu_A(z), \dots, \nu_\Phi(z)$ are then independent zero-mean white-noise processes, with autocorrelation $\mathbb{E}[S_Q(z) S_{Q'}(z')] = \sigma_Q^2 \delta(z-z')$, where $\sigma_Q^2 = \sigma^2 \|\underline{y}_Q\|^2 / \langle \underline{y}_Q, \underline{y}_Q \rangle^2$. All of these variances depend on the soliton amplitude A as well as on the map strength s , and therefore on the propagation distance z . As a result, it is not possible to integrate Eqs. (6) in closed form, even in the case of constant dispersion. If the amplitude deviations are not large, one can approximate $\sigma_A^2, \dots, \sigma_\Phi^2$ as constant. In

this limit, Eqs. (6) can be integrated exactly to give $Q(z) = Q_o + W_Q(z)$ for $Q = A, \Omega$, while

$$T(z) = T_o + \int_0^z \Omega(z') dz' + W_T(z), \quad (7a)$$

$$\Phi(z) = \frac{1}{2} \int_0^z [A^2(z') + \Omega^2(z')] dz' + \int_0^z \Omega(z') S_T(z') dz' + W_\Phi(z), \quad (7b)$$

where $W_Q(z) = \int_0^z S_Q(z') dz'$ is a zero-mean Wiener process with autocorrelation $\mathbb{E}[W_Q(z) W_{Q'}(z')] = \sigma_Q^2 \delta_{QQ'} \min(z, z')$. Unlike other soliton parameters, the mean value of the soliton phase is affected by the noise

$$\mathbb{E}[\Phi(L)] = \frac{1}{2}(A_o^2 + \Omega_o^2)L + \frac{1}{4}(\sigma_A^2 + \sigma_\Omega^2)L^2. \quad (8)$$

Stochastic calculus also yields the variances of the noise-perturbed output soliton parameters as $\text{var}[A(L)] = \sigma_A^2 L$, $\text{var}[\Omega(L)] = \sigma_\Omega^2 L$, $\text{var}[T(L)] = \sigma_T^2 L + \frac{1}{3} \sigma_\Omega^2 L^3$, and

$$\begin{aligned} \text{var}[\Phi(L)] &= (\sigma_\Phi^2 + \Omega_o^2 \sigma_\Omega^2) L + \Omega_o \sigma_T^2 \sigma_\Omega^2 L^2 \\ &+ \frac{1}{3}(A_o^2 \sigma_A^2 + \Omega_o^2 \sigma_\Omega^2) L^3 + \frac{1}{12}(\sigma_A^4 + \sigma_\Omega^4) L^4. \end{aligned} \quad (9)$$

The cubic dependence on the distance of the phase jitter due to the Kerr effect is the Gordon-Mollenauer jitter [11], but note that additional contributions are present. Remarkably, these results are formally identical to those for the NLSE [12]. The dependence of the variance on the soliton amplitude, however, is dramatically different due to the different dependence on A of the norms and inner products [7]. More importantly, these results are not enough to accurately estimate the occurrence of those rare events in which the noise produces large phase deviations, because (i) the prediction for the mean phase is inaccurate, as we show below; (ii) the knowledge of noise-induced means and variances is not enough to estimate behavior in the tails, because not all soliton parameters are Gaussian distributed; and (iii) even if the output probability density functions (PDFs) were Gaussian, extrapolating the results to reach the distribution tails would magnify all uncertainties exponentially, thereby making any prediction meaningless.

IV. MOST LIKELY NOISE-INDUCED PHASE DEVIATIONS

Even though perturbation theory is not enough by itself to predict failure rates, it provides a key tool to implement IS. To successfully apply IS, one must first find the most likely noise realization subject to the constraint of achieving a given parameter change. For additive white Gaussian noise, this problem is solved by minimizing the negative of the argument of the exponential in the noise PDF, namely, the integral $\int |\nu_n(x)|^2 dx$, subject to the constraint $\Delta Q_n = \Delta Q_{\text{target}}$. The solution is [7]

$$\nu_{n, \text{opt}}(t) = \Delta Q_{\text{target}} e^{i\Theta(z)} \underline{y}_Q(t) \langle \underline{y}_Q, \underline{y}_Q \rangle / \|\underline{y}_Q\|^2. \quad (10)$$

To induce a larger-than-normal parameter change, one can then bias the noise by concentrating the MC samples around $\nu_{n, \text{opt}}(x)$. That is, $\nu_{n, \text{biased}}(t) = \nu_{n, \text{opt}}(t) + \nu_n(t)$, where $\nu_{n, \text{opt}}(t)$ is given above and $\nu_n(t)$ is unbiased.

Once the most likely noise realization that produces a given parameter change ΔQ_n at each map period is known,

one must also find the most likely way to distribute a total parameter change ΔQ_{tot} at the output among all map periods. In principle, when seeking large phase changes, one must bias an appropriate combination of all linear modes. Among the terms in the right-hand side of Eq. (6), however, changes in Ω^2 and $\langle e^{-i\theta} y_T, S \rangle \Omega$ are second order in the noise, while changes in A^2 are first order in the noise, because $\Omega_o = 0$ while $A_o \neq 0$. We thus introduce the auxiliary quantity $\phi(z)$ such that $d\phi/dz = A^2/2 + \nu_{\phi}(z)$ and $\phi(0) = \Phi_o$ and consider the optimal biasing problem for $\phi(z)$. In the continuum approximation, the biasing function is then

$$b(t, z) = \dot{A} y_A \langle y_A, y_A \rangle / \|y_A\|^2 + (\dot{\phi} - A^2/2) y_{\phi} \langle y_{\phi}, y_{\phi} \rangle / \|y_{\phi}\|^2. \quad (11)$$

[The direct phase biasing is not given by $\dot{\phi} z_a$, but rather by $(\dot{\phi} - A^2/2) z_a$.] Minimizing the sum of the L_2 norm of this biasing function over all amplifiers is equivalent to finding functions $A(z)$ and $\phi(z)$ that minimize the functional

$$J[A, \phi] = \int_0^L [(1/\sigma_A^2) \dot{A}^2 + (1/\sigma_{\phi}^2) (\dot{\phi} - A^2/2)^2] dz. \quad (12)$$

The Euler-Lagrange equations associated with $J[A, \phi]$ yield

$$\dot{\phi} - A^2/2 = c\sigma_{\phi}^2, \quad (13a)$$

$$2\ddot{A}(1/\sigma_A^2) + \dot{A}^2(\partial/\partial A)(1/\sigma_A^2) + c^2(\partial/\partial A)(\sigma_{\phi}^2) + 2cA = 0, \quad (13b)$$

where c is a Lagrange multiplier. The solution of the system composed of Eq. (12), together with the boundary conditions $A(0) = A_o$, $\phi(0) = \dot{A}(L) = 0$, and $\phi(L) = \phi_{\text{target}}$, determines the optimal amplitude and the phase paths around which one must bias the ISMC simulations. [The condition $\dot{A}(L) = 0$ applies because amplitude changes at $z = L$ do not produce phase changes.] This system can be integrated numerically using relaxation methods or numerical continuation software. Different output phases can be targeted by solving the system for different values of c , which determines the amount of biasing being applied ($c = 0$ yields no bias). Equations (11), (12), (13a), and (13b) reduce to known results in the case of constant dispersion [4, 13]. But unlike the constant-dispersion case (and unlike the case of time biasing), here the direct phase biasing is not constant in z . Physically, this is a consequence of the different way in which noise is translated into phase jitter in the DMNLSE by way of the linear modes.

V. ISMC SIMULATIONS

We now discuss ISMC simulations aimed at computing the PDF of the soliton phase at the output. To quantify larger-than-normal phase deviations, we perform the following steps at each map period: (i) recover the underlying DMS from the noisy signal; (ii) obtain the linear modes and adjoint modes of the linearized DMNLSE around the given DMS; and (iii) generate an unbiased noise realization, shift its mean with the appropriately scaled adjoint modes, and update the likelihood ratios [7]. We then add the noise to the pulse, propagate the noisy signal to the next map period, and repeat this process until the signal reaches the output. For each noise realization, the full DMNLSE is used to propagate the

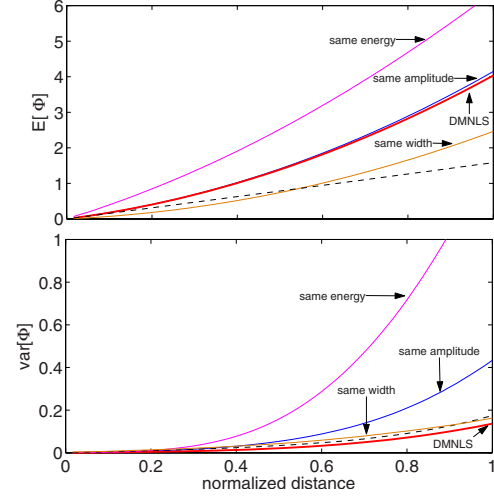


FIG. 1. (Color online) Mean (top) and variance (bottom) of the soliton phase as reconstructed with standard MC simulations. Thick (red) lines, DMNLSE. Also shown for comparison are results for constant-dispersion NLSE solitons with the same amplitude (blue) as the DMS, same energy (magenta), and same width (orange). Dashed lines, predictions from perturbation theory.

signal. (The linearized DMNLSE is only used to guide IS via its modes.) Even though the noise-induced DMS parameter changes at each map period are small, the accumulation of these changes often results in a significantly distorted output signal.

We choose system parameters based on realistic values for optical fiber communications. Typical values of system parameters for fs lasers can be obtained from Ref. [14]. We consider a piecewise constant dispersion map, with equal-length normal and anomalous dispersion sections and local dispersion coefficients of 23.27 and -22.97 ps²/km, resulting in an average dispersion of 0.15 ps²/km. We set the unit time to 17 ps, corresponding to $\bar{d} = 1$ and $s = 4$, and we use the resulting dispersion length of 1923 km to normalize distances. We consider a transmission distance of 6000 km (or $L = 3.1201$) and amplifiers spaced 100 km apart, for a total of $N_a = 60$ with dimensionless spacing $z_a = 0.052$, and we set the map period to be aligned with them. We take a nonlinear coefficient of 1.7 (W km)⁻¹, a peak power of 3.51 mW, a loss coefficient of 0.25 dB/km, a spontaneous emission factor of 1.65, resulting in a dimensionless noise variance $\sigma^2 = 1.873 \times 10^{-3}$ and an optical signal-to-noise ratio of 9.3 dB. We normalize pulse powers with the power needed to have $\bar{g} = 1$, namely, 3.51 mW. Finally, we take input pulses to have unit peak amplitude, resulting in $A_o = 1$.

VI. NUMERICAL RESULTS AND DISCUSSION

Figure 1 shows the numerically reconstructed phase mean and variance as functions of distance for the DMNLSE, as well as the corresponding values for constant-dispersion NLSE solitons with same mean, amplitude, or energy as the DMS, plus the predictions of perturbation theory. Note that the DMS has the lowest variance of all. (The constant-dispersion NLSE soliton with same width as the DMS has a much lower energy, which makes it much more susceptible

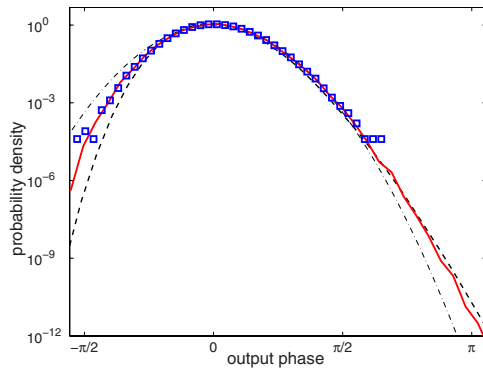


FIG. 2. (Color online) PDF of output phase. Solid line, ISMC simulation of DMNLSE with 50 000 samples. Squares, standard MC simulation of the NLSE+DM with 250 000 samples. Dashed curve, ISMC simulation of the noise-driven SDEs (6). Dotted-dashed curve, a Gaussian PDF with variance given by Eq. (9).

to Gordon-Haus jitter.) Note that the means and the variances of the numerically reconstructed phase depend dramatically on the particular definition of phase used in the simulations. Hence, consistency is crucial to ensure agreement between theory and simulations. Here, the phase of a noisy pulse is defined (both in the theory and in the numerics) as that of the underlying DMS (obtained as in [7]).

A significant discrepancy is evident between analytical and numerical results for the mean phase. No satisfactory explanation currently exists for this effect, which also occurs for the NLSE [13]. It is likely to depend on a failure of SPT and/or from second-order effects. (Numerical results show that the discrepancy also depends on the computational noise bandwidth.) On the other hand, the analytical prediction for the variance agrees very well with the numerical results, both for the NLSE and the DMLNSE.

Figure 2 shows the PDF of the DMS output phase as computed from ISMC simulations of the DMNLSE (2), standard MC simulations of the NLSE+DM (1), plus a Gaussian distribution with variance given by perturbation theory and a PDF obtained from direct ISMC simulations of the SDEs (6). The ISMC results collect samples generated with a few biasing targets, using multiple ISs [15] to properly combine the data. The PDFs from both the DMNLSE and the NLSE

clearly deviate from Gaussian, but they agree very well with each other as far down in probability as the unbiased MC simulations can reach. Conversely, while the Gaussian approximation agrees well near the peak of the PDF, for deviations from the mean phase of π or more (a value that is relevant for fs lasers) it is off by several orders of magnitude. Similarly, the SDEs obtained from perturbation theory fail to accurately reproduce the full dynamics of the soliton phase at lower-than-average values of phase. Remarkably, however, ISMC simulations guided by perturbation theory yield the correct phase behavior.

Importantly, results from the noise-perturbed DMNLSE and NLSE+DM agree *pathwise*, not just in the overall PDFs at the output. That is, they agree for each noise realization as a function of distance. These results, which are surprising given the “softness” of the phase and the complexity of the system (nonlinearity, dispersion, noise, large deviations etc.), provide further confirmation of the validity and the robustness of the DMNLSE in capturing the essential dynamics of DM systems. Its usefulness is also increased by the availability of tools such as the perturbation theory presented here, an analog of which is lacking for the NLSE+DM.

Similar dynamics should also arise for nonsolitonic pulses, but the analysis for that case will be more complicated because generic pulses do not preserve a flat phase across their temporal profile upon propagation.

An important question is also whether these results can be used in fs lasers in order to quantify the probability of the occurrence of phase slips in optical atomic clocks. Since gain and loss play an obvious role in lasers, one could expect that it will be necessary to derive a perturbation theory for the nonconservative version of the DMNLSE that was derived as a model for fs lasers [16]. Since the DMNLSE itself provides a surprisingly good quantitative description of these lasers [14], however, whether or not such an extension will indeed be necessary remains at present an open question.

ACKNOWLEDGMENTS

We thank S. T. Cundiff and W. L. Kath for many insightful discussions. This work was partially supported by NSF under Grants No. DMS-0112069, No. DMS-0506101, and No. DMS-0757527.

[1] L. F. Mollenauer and J. P. Gordon, *Solitons in Optical Fibers: Fundamentals and Applications* (Academic Press, New York, 2006).
 [2] J. Ye and S. T. Cundiff, *Femtosecond Optical Frequency Comb: Principle, Operation and Applications* (Springer, New York, 2004).
 [3] R. O. Moore *et al.*, *Opt. Lett.* **28**, 105 (2003).
 [4] R. O. Moore *et al.*, *SIAM Rev.* **50**, 523 (2008).
 [5] E. Spiller *et al.*, *IEEE Photonics Technol. Lett.* **17**, 1022 (2005).
 [6] A. Tonello *et al.*, *IEEE Photonics Technol. Lett.* **18**, 886 (2006).

[7] J. Li *et al.*, *Phys. Rev. A* **75**, 053818 (2007).
 [8] M. J. Ablowitz and G. Biondini, *Opt. Lett.* **23**, 1668 (1998).
 [9] I. R. Gabitov and S. K. Turitsyn, *Opt. Lett.* **21**, 327 (1996).
 [10] M. J. Ablowitz *et al.*, *Opt. Lett.* **29**, 1808 (2004).
 [11] J. P. Gordon and L. F. Mollenauer, *Opt. Lett.* **15**, 1351 (1990).
 [12] K.-P. Ho, *J. Opt. Soc. Am. B* **21**, 266 (2004).
 [13] E. T. Spiller and W. L. Kath, *SIAM J. Appl. Dyn. Syst.* **7**, 868 (2008).
 [14] Q. Quraishi *et al.*, *Phys. Rev. Lett.* **94**, 243904 (2005).
 [15] G. Biondini *et al.*, *IEEE J. Lightwave Technol.* **22**, 1201 (2004); **24**, 1065 (2006).
 [16] G. Biondini, *Nonlinearity* **21**, 2849 (2008).